Multidisciplinary Materials Chronicles, 2024, Vol. 1, Iss. 1, 19-29

DOI: 10.62184/mmc.jmmc110020242

Research Article

SCIENCE PARK PUBLISHER

Multidisciplinary Materials Chronicles

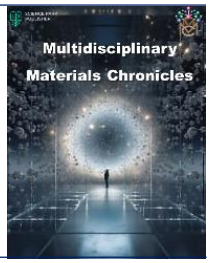

Evaluating the Effectiveness of Tellurium-Molybdenum Oxide Glass Systems for Radiation Shielding Protection

Shams A. M Issa[1,2], Antoaneta Ene[3], Hesham M. H. Zakaly[2,4,*]

[1] Department of Physics, Faculty of Science, University of Tabuk, Tabuk, Saudi Arabia

[2] Physics Department, Faculty of Science, Al-Azhar University, Assiut, 71452, Egypt

[3] INPOLDE Research Center, Department of Chemistry, Physics and Environment, Faculty of Sciences and Environment, Dunarea de Jos University of Galati, 47 Domneasca Street, 800008 Galati, Romania

[4] Institute of Physics and Technology, Ural Federal University, 19 Mira St, 620002, Yekaterinburg, Russia

Received: 15, 02, 2024; Accepted: 31, 03, 2024; Published: 22, 04, 2024

Abstract

The present investigation examined TeO_2–MeO_3 glasses with different compositions for their ability to absorb γ-rays using the Phy-X and FLUKA Code, respectively. The study covered energies ranging from 0.015 to 15 MeV, where several parameters such as effective atomic number (Z_{eff}), free path mean (G_{MFP}), mass attenuation coefficient (G_{MAC}), macroscopic cross-section (G_{LAC}), and half-value levels were analyzed (G_{HVL}). Glass composite composed of 80% TeO_2 and 20% MoO_3 was found to have the lowest G_{LAC} content among the tested samples. G_{HVL} = 0.055 cm was the half-value of the $80TeO_2$–$20MoO_3$ glasses when they were subjected to 80 keV gamma-rays. It is anticipated that the G_{MFP} of the investigated materials ranges from 0.004 to 0.005 cm when subjected to 100 keV gamma-rays. It was said that the increase in Z_{eff} may be attributed to an increased quantity of electrons that were accessible for interaction with photons, resulting in a decreased probability of gamma rays passing through the shielding material. The cumulative impact of these findings demonstrates that specific glass compositions, particularly those that include Tellurium, have the potential to be used as excellent radiation shielding materials. These materials are becoming more important for providing efficient radiation protection in various industries and applications, including medical imaging, nuclear power, and space exploration.

Keywords: Tellurium; molybdenum; Gamma ray shielding; PHY-X; FLUKA

1. Introduction

Nuclear technology has ushered in a new era of innovation, profoundly influencing human activities across multiple sectors, including medical therapeutics, agricultural practices, research diagnostics, industrial applications, and sustainable energy generation through nuclear reactors. The advent of such diverse applications has underscored the criticality of identifying and utilizing suitable shielding materials to safely contain the various forms of radiation emanating from these technologies. In particular, within the operational environments of nuclear reactors, there is an essential need for materials that can effectively insulate against both gamma rays and neutrons [1–3]. Concrete has been the material of choice for radiation shielding due to its widespread availability and relative effectiveness. However, the protective quality of concrete is inherently limited

DOI: 10.62184/mmc.jmmc110020242

Research Article

by its hydrophilic nature. Fluctuations in moisture content can compromise its structural integrity, leading to variations in strength and density that diminish its shielding capacity [4]. Despite offering reasonable levels of protection, traditional shielding materials, such as concrete, metals, polymers, and even lead, encounter limitations due to thermal instability, susceptibility to compositional changes, lack of transparency, and a constrained scope of utility.

In the quest for more versatile shielding solutions, the industry focuses on developing transparent materials that can offer robust defense against gamma and X-rays. Such materials are in high demand within nuclear medicine and diagnostic imaging [5–7]. Addressing this need, the production process has been geared towards glass systems that integrate high levels of transparency with efficient absorption of radiation gases [8]. Glasses enriched with heavy metal oxides, notably lead oxide (PbO), are increasingly favored for such applications. This preference is attributed to their inherent properties, such as high polarizability, lower melting points, and superior refractive indices, in addition to their transparency, and chemical and thermal robustness [9].

In pursuing advancing radiation protection technologies, this investigation employs FLUKA Simulation and Phy-x/PSD simulation software to meticulously evaluate the radiation shielding characteristics of newly developed glass models. The study focuses on determining the glass models' performance in several key shielding capacities, including gamma mass attenuation coefficient (G_{MAC}), linear attenuation coefficient (G_{LAC}), half-value layer (G_{HVL}), mean free path (G_{MFP}), tenth value layer (G_{TVL}), and effective atomic number (Z_{eff}) [10–12]. The spotlight of current research interest is on the Tellurium–Molybdenum Oxide Glass (Te-Mo glass) systems, which are being examined for their potential as superior radiation shields. This burgeoning interest is propelled by the urgent necessity for effective radiation protection materials that are not only technologically adept in providing exceptional shielding against harmful radiation but also maintain their beneficial attributes amidst the escalating advancements in medical imaging, energy production, and aerospace exploration.

2. Materials and Method

2.1. Materials

The study conducted a theoretical examination of the gamma-ray (γ-ray) shielding capabilities of four different glass materials. These materials are identified by their chemical compositions: 50% tellurium dioxide (TeO_2) and 50% molybdenum trioxide (MoO_3), 60% TeO_2 and 40% MoO_3, 70% TeO_2 and 30% MoO_3, and 80% TeO_2 and 20% MoO_3[13]. For convenience, these compositions are abbreviated as 50Te, 60Te, 70Te, and 80Te, respectively. Computational analyses were performed on these materials to evaluate various γ-ray shielding characteristics. Details about these glass samples, including their assigned codes, densities, and molar volumes, are provided in **Table 1**. The table describes a study focusing on the efficiency of certain glass materials in shielding against γ-rays. The materials are mixtures of tellurium dioxide and molybdenum trioxide in varying proportions. Each material's effectiveness in γ-ray shielding could be influenced by its composition, as the density and molar volume of the glass are likely to impact its shielding performance. The density of the materials appears to increase as the proportion of TeO_2 increases, suggesting that a higher concentration of TeO_2 in the glass composition results in a denser material. This trend could be relevant for γ-ray shielding since denser materials generally provide better attenuation of high-energy photons like γ-rays. Conversely, the molar volume decreases as the TeO_2 content increases, which correlates with the increasing density – as density increases, molar volume typically decreases, given that molar volume is a measure of the volume occupied by one mole of a substance. The incremental changes in the glass composition reflected by the glass code from 50Te to 80Te indicate a systematic variation in the materials' properties, which are likely being studied to understand how these variations affect γ-ray shielding efficiency. The research might be looking to optimize glass compositions for the most effective γ-ray shielding, balancing between density, molar

DOI: 10.62184/mmc.jmmc110020242

Research Article

volume, and potentially other factors like cost, durability, and ease of manufacture.

Table 1. The Chemical Composition and Density(g/cm^3) of Investigated Glass Samples.

No.	Glasses composition	Glass code	Density (g/cm^3)	Molar Volume (cm^3/mol)
1.	$50TeO_2$-$50MoO_3$	50Te	4.858	31.24
2.	$60TeO_2$-$40MoO_3$	60Te	5.018	30.56
3.	$70TeO_2$-$30MoO_3$	70Te	5.176	29.93
4.	$80TeO_2$-$20MoO_3$	80Te	5.251	29.80

2.2. Shielding Simulation

The assessment of glass compositions infused with tellurium and molybdenum oxides for radiation protection necessitates rigorous simulation analysis due to the hazardous nature of empirical γ-ray interaction studies. FLUKA simulation software, [14–16] collaboratively developed by CERN along with various other research entities, is at the forefront of this analysis, providing a virtual environment for particle interaction and propagation in matter. These simulations serve an essential role in high-energy physics, radiation protection, engineering, and medical physics, with their reliability bolstered by comprehensive validations against a broad spectrum of experimental data.

FLUKA is a particle physics Monte Carlo simulation package, integral for simulating complex interactions of particles with matter. The software's robustness is evidenced through numerous validations across diverse energies and materials, as explored in seminal reviews and in-depth discussions concerning its underpinning physical models [15, 17]. The precision with which FLUKA models the interactions between γ-rays and shielding materials is of particular relevance to the study of Tellurium-Molybdenum Oxide Glass Systems.

Figure 1 demonstrates the sophisticated simulation setup employed to evaluate the efficacy of various glass compositions in attenuating γ-rays. Utilizing the FLUKA Code, lauded for its advanced computational capabilities in particle physics simulations, alongside Phy-X software, this approach facilitates a granular and comprehensive analysis of γ-ray interactions. The simulation's framework managed through the FLAIR interface, depicts the spatial arrangement and geometrical specifics of the glass samples according to the detection apparatus. As an intuitive graphical user interface, FLAIR significantly streamlines the preparatory and analytical phases of simulation processes.

Despite the demonstrable precision of FLUKA simulations, it is imperative to recognize the intrinsic limitations and assumptions that accompany any simulated model. The veracity of simulations is contingent upon the model's adherence to physical reality and the precision of the defined input parameters. Variabilities inherent to real-world conditions, such as fluctuations in material properties or inconsistencies in manufacturing practices, may not be entirely captured within the simulation's parameters, thus necessitating the need for empirical validation. The definitive verification of simulation accuracy lies in experimental comparison, which is instrumental in augmenting the robustness of the computational findings, particularly within the domain of radiation shielding materials. FLUKA simulations provide a substantial foundation for theoretical inquiry and preclinical investigation, offering intricate insights into the interaction dynamics of γ-rays with potential shielding materials.

Multidisciplinary Materials Chronicles, 2024, Vol. 1, Iss. 1, 19-29

DOI: 10.62184/mmc.jmmc110020242

Research Article

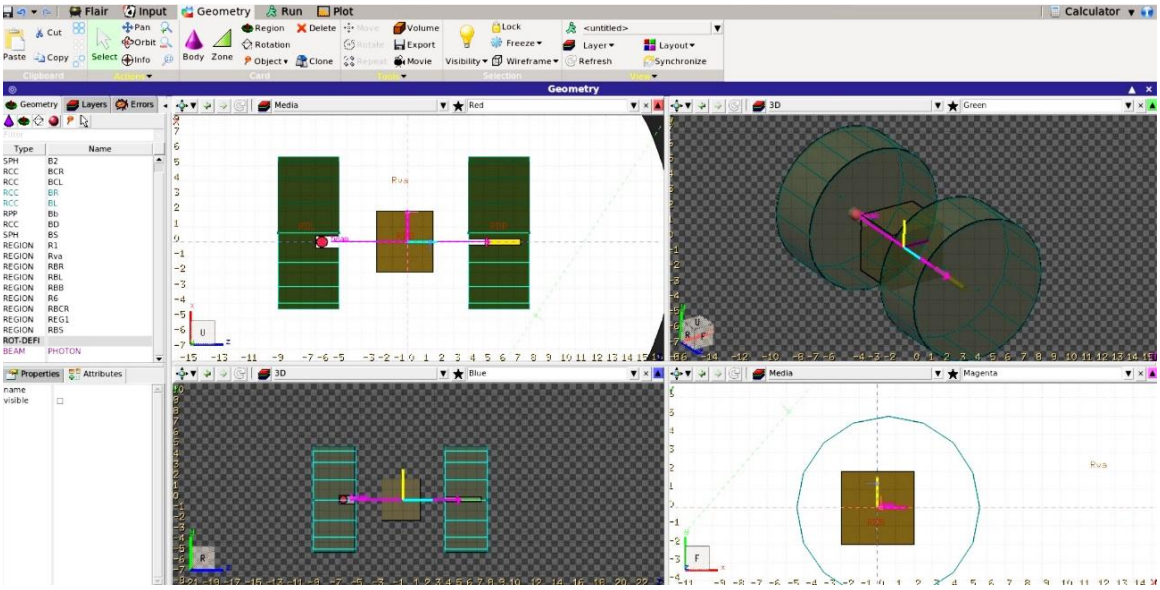

Figure 1. Simulation process geometry setup using FLAIR interface.

3. Results and Discussions

3.1. Physical Properties

Figure 2 illustrates the variation in density and molar volume for glass compositions ranging from 50Te to 80Te. As depicted in **Figure 2a**, there is an upward trend in density for the glass samples from 50Te to 80Te, with values ascending from 4.858 to 5.251 g/cm^3. Conversely, **Figure 2b** demonstrates a downward trajectory in molar volume for the same range of glass samples, decreasing from 31.24 cm^3/mol to 29.80 cm^3/mol. The increase in density is likely a consequence of the augmented Tellurium content, which escalates from 50 to 80 mol%. A reduction in molar volume is observed due to the inverse relationship between density and molar volume expressed by the equation $\rho = M/V$. This correlation implies that with the increment in glass density, there is a corresponding enhancement in material compactness, culminating in a diminished molar volume for the glass samples.

3.2. Shielding properties

3.2.1. Macroscopic Cross-section

Following the Beer-Lambert law, which is represented by the equation (1), the rate at which the intensity of radiation scattering and absorption that is transmitted via shielding materials (mixtures, alloys, and compounds) is measured expressed by [18]:

$$I = I_o \; e^{-G_{LAC}\, t} \qquad (1)$$

where I_o represents the intensity of incident photons, and I stands for the intensity of transmitted photons. With the help of Phy-X programs and the FLUKA Code, Table 2 illustrates the parameters that were determined by G_{LAC} and how they changed in response to the energy of the incoming photon. It can be seen from **Table 2** that the results of the FLUKA simulations and the Phy-X analysis were in agreement for each sample. Additionally, the findings demonstrate that the G_{LAC} decreases as the amount of energy increases, which is a consequence of the high penetrating strength of radiation [19]. At the energy levels of 40 keV, sharp absorption edges were seen in Table 2 for all samples. This indicates the existence of Te elements, which are represented by the K-edge.

Multidisciplinary Materials Chronicles, 2024, Vol. 1, Iss. 1, 19-29

DOI: 10.62184/mmc.jmmc110020242

Research Article

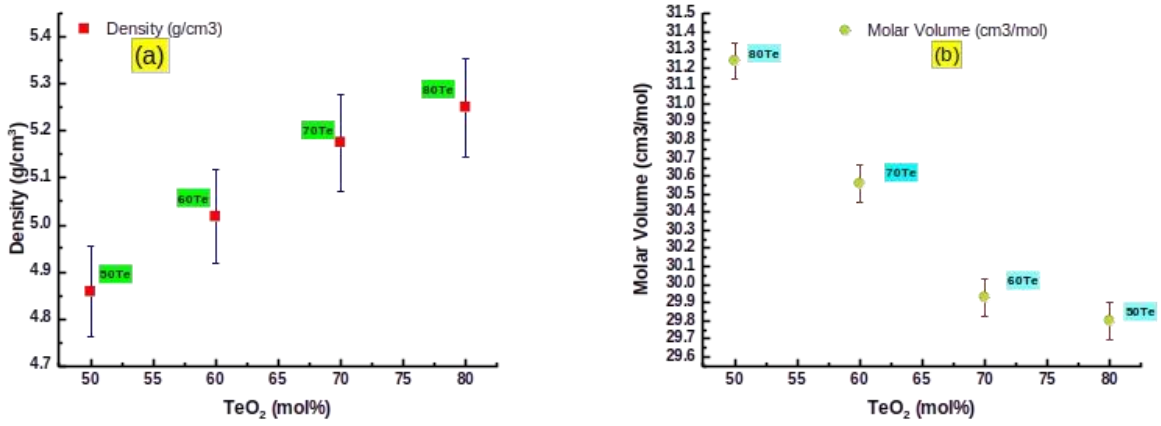

Figure 2. (a) Density and (b) molar volume change with sample concentration.

Table 2. Linear attenuation coefficient (G_{LAC}, cm^{-1}) of the glass samples.

E	50Te		60Te		70Te		80Te	
(MeV)	Phy-X	FLUKA	Phy-X	FLUKA	Phy-X	FLUKA	Phy-X	FLUKA
0.015	149.861	150.460	165.363	166.025	181.249	181.974	194.493	195.271
0.020	171.060	171.744	159.645	160.283	147.441	148.031	132.447	132.977
0.030	59.717	59.955	55.502	55.724	51.002	51.206	45.530	45.712
0.040	62.362	62.611	68.303	68.577	74.383	74.681	79.367	79.684
0.050	34.465	34.603	37.796	37.947	41.206	41.370	44.009	44.185
0.060	21.184	21.269	23.246	23.339	25.357	25.459	27.096	27.204
0.080	9.875	9.914	10.830	10.874	11.808	11.855	12.612	12.663
0.100	5.559	5.581	6.083	6.108	6.620	6.646	7.058	7.087
0.150	2.147	2.155	2.327	2.336	2.510	2.520	2.656	2.667
0.200	1.231	1.236	1.319	1.324	1.408	1.414	1.477	1.483
0.300	0.691	0.694	0.728	0.731	0.765	0.768	0.790	0.793
0.400	0.521	0.523	0.543	0.545	0.566	0.568	0.579	0.581
0.500	0.438	0.440	0.455	0.456	0.471	0.473	0.480	0.482
0.600	0.388	0.389	0.401	0.403	0.414	0.416	0.421	0.422
0.800	0.326	0.327	0.336	0.337	0.346	0.347	0.350	0.352
1.000	0.287	0.288	0.295	0.297	0.304	0.305	0.307	0.308
1.500	0.231	0.232	0.238	0.239	0.244	0.245	0.246	0.247
2.000	0.203	0.204	0.209	0.210	0.215	0.215	0.217	0.218
3.000	0.176	0.177	0.182	0.182	0.187	0.188	0.190	0.190
4.000	0.165	0.165	0.170	0.171	0.176	0.177	0.179	0.180
5.000	0.160	0.160	0.166	0.166	0.171	0.172	0.175	0.175
6.000	0.158	0.158	0.164	0.164	0.170	0.171	0.173	0.174
8.000	0.158	0.159	0.165	0.166	0.172	0.172	0.176	0.176
10.000	0.162	0.162	0.169	0.169	0.176	0.177	0.180	0.181
15.000	0.173	0.173	0.181	0.182	0.189	0.190	0.195	0.195

Multidisciplinary Materials Chronicles, 2024, Vol. 1, Iss. 1, 19-29
DOI: 10.62184/mmc.jmmc110020242

Research Article

The results of a comparative study of G_{LAC} vs. energy for each of the samples are shown in **Table 2.** Since G_{LAC} is based on density, 80Te demonstrates the most outstanding G_{LAC} value due to its greater density. Table 2 also indicates that 50Te has the lowest G_{LAC}, another point of interest. According to the theory that the G_{LAC} lowers as density falls, this is compatible with the above idea.

3.2.2. Mass Attenuation Coefficient

To evaluate the mass-attenuation parameter (G_{MAC}), which is the ratio between the G_{LAC} and the density of the samples, equation (2) is used:

$$G_{MAC}=W_i\times(G_{MAC})_I \qquad (2)$$

Figure 3 illustrates the G_{MAC} value calculated using FLUKA at several different energies. As a result of the fact that the mass attenuation coefficient is independent of density and is reliant on both the elemental composition and the atomic number of the element, it offers crucial insights into how the shielding qualities of a material may be adjusted by adjusting the nuclear configuration of a component. In addition, **Figure 3** presents the calculated G_{MAC} values over a range of photon energies, as determined using the FLUKA simulation software. G_{MAC}, independent of material density, is a fundamental property that reveals the intrinsic ability of a substance to attenuate gamma radiation. It primarily depends on the elemental composition and the atomic number of the constituents within the material.

G_{MAC} is an invaluable metric for assessing how modifications in a material's elemental makeup can enhance its protective qualities in radiation shielding. The plot shows that the G_{MAC} decreases with increasing photon energy, which is consistent with the general behavior of photon attenuation in the matter. This trend reflects the dominant interaction mechanisms at different energy levels: the photoelectric effect at low energies, Compton scattering at intermediate energies, and pair production at high energies. The figure shows that the sample labeled as 80Te exhibits the highest G_{MAC} values across the studied energy spectrum. This suggests that the 80Te sample, with its higher proportion of Tellurium (which has a more significant atomic number than molybdenum), presents a more effective gamma shielding material.

The higher atomic number correlates with greater photon interaction cross-sections, thereby providing superior attenuation due to increased photoelectric absorption and other mechanisms. Such insights are crucial for designing materials for radiation shielding applications, particularly in fields where precise control over radiation exposure is necessary, such as nuclear medicine and diagnostics. By understanding the relationship between G_{MAC} and photon energy, researchers and engineers can better select and design materials that balance transparency with effective radiation absorption, ultimately leading to safer and more efficient use of nuclear technology.

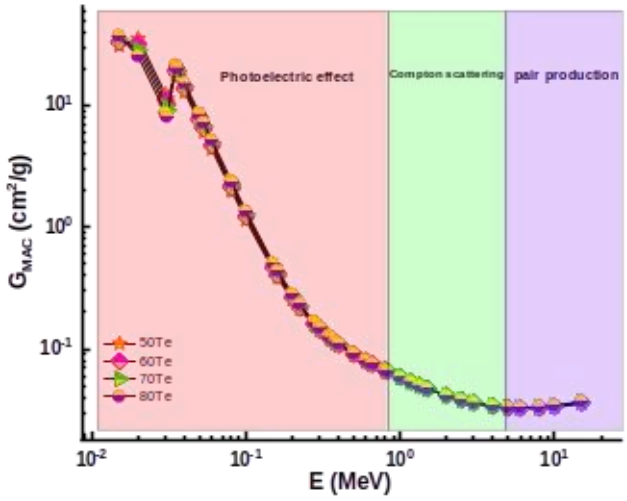

Figure 3. Analysis of G_{MAC} for all samples versus photon energy.

3.2.3. Half-Value-Layer (G_{HVL})

When referring to the thickness of shielding materials capable of lowering radioactive quantities, the term G_{HVL} is used, expressed by equation (3) [20].

$$G_{\mathrm{HVL}} = \frac{ln(2)}{G_{LAC}} \qquad (3)$$

As seen in **Figure 4**, an inverse relationship exists between the G_{HVL} and G_{LAC} values. Furthermore, it is clear from **Figure 4** that the G_{HVL} values progressively grow as the photon energy

Multidisciplinary Materials Chronicles, 2024, Vol. 1, Iss. 1, 19-29
DOI: 10.62184/mmc.jmmc110020242

Research Article

levels rise. This indicates that the shielding material must have a greater thickness to reduce the amount of Half-Value energy radiation [21]. Furthermore, it is evident from **Figure 5** that a thickness that falls within the range of a few centimeters may significantly diminish the intensities of X-rays and γ- rays. The fact that the investigated glass samples 50Te, 60Te, 70Te, and 80Te had G_{HVL} values of 0.020, 0.018, 0.017, and 0.016 cm, respectively, at an energy of 50 keV, illustrates the relevance of the potential uses of these glasses.

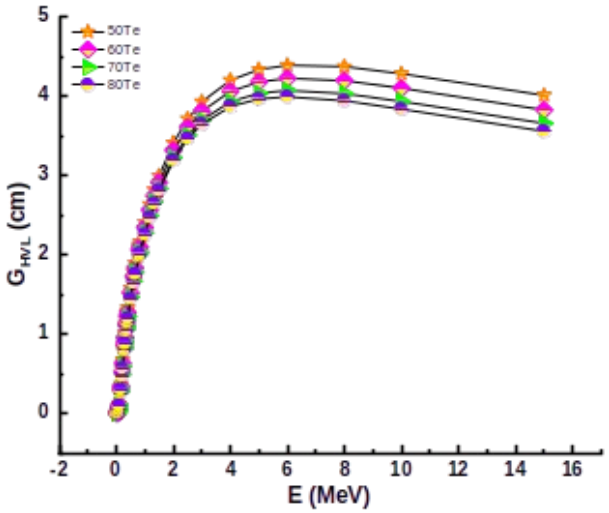

Figure 4. Half-Value layers (G_{HVL}) using FLUKA code simulation for glass samples versus photon energy.

3.2.4. Mean-Free-Path (G_{MFP})

During the process of a photon traveling through a substance, the photon may interact with either the atomic nuclei or the electrons of the material. Because of this interaction, the direction of motion of photons is altered to a large extent. G_{MFP} is the term used to describe the average route that photon travels through the material without encountering anything, being expressed by the equation (4) [22].

$$G_{\text{MFP}} = \frac{1}{G_{LAC}} \qquad (4)$$

In **Figure 5**, we notice a rise in the average distance separating subsequent contacts. As the amount of energy grows, the G_{MFP} goes from a lower value to a larger one, eventually reaching a point where it is saturated and remains constant for all four samples. The 80Te sample has the most excellent density compared to other samples because Tellurium has a more significant molar fraction and a higher Z-number. As a result, the G_{MFP} of this sample is relatively low compared to different samples. 0.180, 0.164, 0.151, and 0.142 cm are the values of the G_{MFP} for our sample that was tested at an energy of 100 keV.

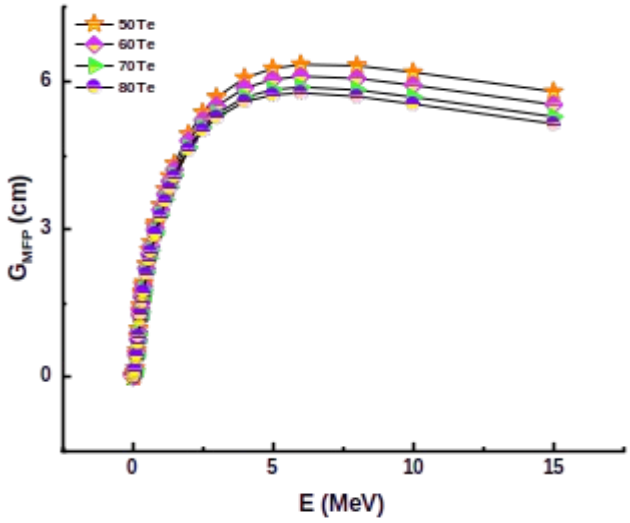

Figure 5. Mean-Free-Path (G_{MFP}) for all glass samples versus photon energy.

3.2.5. Effective atomic number (Z_{eff})

The value of the GMAC that is obtained from the FLUKA simulation is used to assess the atomic cross section (σ_a) and the electronic cross section (σ_e) by using equations (5) and (6), respectively [23].

$$\sigma_a = \frac{G_{MAC}N}{N_A} \qquad (5)$$

$$\sigma_e = \frac{f_i G_{MAC} N_i}{N_A Z_i} \qquad (6)$$

In addition, these values are then used to determine the effective atomic number (Z_{eff}) of the glass being investigated, given by the equation (7) [24].

$$Z_{eff} = \frac{\sigma_a}{\sigma_e} \qquad (7)$$

DOI: 10.62184/mmc.jmmc110020242

Research Article

Figure 6, illustrates the relationship between the effective atomic number (Z_{eff}) of the glass samples and photon energy. Z_{eff} is a measure of the overall shielding effectiveness of a material, representing an average atomic number that quantifies the composite effect of all the elements in the material on radiation attenuation [25]. The figure shows that Z_{eff} varies with photon energy, displaying a U-shaped curve typical of photon interaction processes. The increase in Z_{eff} with photon energy at low energies indicates the photoelectric effect being the dominant interaction mechanism. At intermediate energies, Z_{eff} decreases as Compton scattering becomes more prevalent. Z_{eff} rises again at the highest energies because pair production becomes the significant interaction process. This behavior reflects the increase in available electrons for photon interaction, which leads to a higher probability of photon attenuation by the material. In practical terms, a higher Z_{eff} at a given energy means that the material is more effective at blocking or attenuating photons at that energy level, which is crucial for designing materials for specific radiation shielding applications.

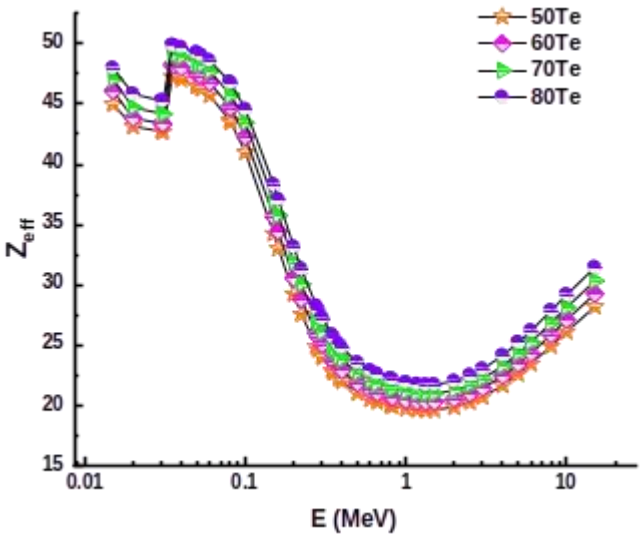

Figure 6. Effective atomic number (Z_{eff}) of glass samples versus photon energy.

4. Conclusion

This study scrutinized glass compositions containing Tellurium and molybdenum oxide for their capabilities as radiation shielding materials. Through the application of FLUKA simulations and Phy-X/PSD analytical tools, the investigation focused on determining fundamental shielding properties, such as Gamma Mass Attenuation Coefficient (G_{MAC}), Gamma Linear Attenuation Coefficient (G_{LAC}), Mean Free Path (G_{MFP}), Half Value Layer (G_{HVL}), and Effective Atomic Number (Z_{eff}), across a photon energy range of 0.015 to 15 MeV. The research revealed a decline in G_{LAC} with an escalation in energy levels due to radiation's formidable penetrating prowess. An evident absorption edge was detected at the potential energy threshold of 40 keV for all glass samples, attributable to the K-edge absorption associated with tellurium elements. Notably, the 80Te sample distinguished itself by offering superior γ-ray shielding effectiveness, as suggested by its minimal G_{HVL} values. This heightened performance is ascribed to the more significant molar fraction of Tellurium and

DOI: 10.62184/mmc.jmmc110020242

Research Article

the consequent increase in the sample's effective atomic number (Z_{eff}) compared to the other samples evaluated. The G_{MFP} values demonstrated an initial decrease with rising energy levels, eventually reaching a plateau, indicative of a consistent saturation point across all four types of glass samples. The 80Te sample, with its maximal density, predictably exhibited a reduced G_{MFP}, underscoring its enhanced shielding efficacy.

Acknowledgments

H.M.H Zakaly thanks the Ministry of Science and Higher Education of the Russian Federation (Ural Federal University Program of Development within the Priority-2030 Program) is gratefully acknowledged.

Conflicts of Interest

The authors declare no competing interests.

Author Information

Corresponding Author: Hesham M. H. Zakaly*

E-mail: h.m.zakaly@gmail.com

Data Availability

The present authors declare that the work data and materials are available.

References

[1] K.J. Singh, S. Kaur, R.S. Kaundal, Comparative study of gamma ray shielding and some properties of PbO-SiO_2-Al_2O_3 and Bi_2O_3-SiO_2-Al_2O_3 glass systems, Radiat. Phys. Chem. 96 (2014) 153–157. https://doi.org/10.1016/j.radphyschem.2013.09.015.

[2] M.G. El-Samrah, M.A.E. Abdel-Rahman, R.M. El Shazly, Effect of heating on physical, mechanical, and nuclear radiation shielding properties of modified concrete mixes, Radiat. Phys. Chem. 153 (2018) 104–110. https://doi.org/10.1016/J.RADPHYSCHEM.2018.09.018.

[3] A.M.A. Mostafa, H.M. Zakaly, S.A. Al-Ghamdi, S.A. Issa, M. Al-Zaibani, R.M. Ramadan, E.F. El Agammy, PbO–Sb_2O_3–B_2O_3–CuO glassy system: Evaluation of optical, gamma and neutron shielding properties, Mater. Chem. Phys. 258 (2021) 123937–123947. https://doi.org/10.1016/j.matchemphys.2020.123937.

[4] M. Kurudirek, Y. Özdemir, Ö. Şimşek, R. Durak, Comparison of some lead and non-lead based glass systems, standard shielding concretes and commercial window glasses in terms of shielding parameters in the energy region of 1keV–100GeV: A comparative study, J. Nucl. Mater. 407 (2010) 110–115. https://doi.org/10.1016/j.jnucmat.2010.10.007.

[5] M.S. Al-Buriahi, S. Alomairy, C. Mutuwong, Effects of MgO addition on the radiation attenuation properties of 45S5 bioglass system at the energies of medical interest: An in silico study, J. Aust. Ceram. Soc. 57 (2021) 1107–1115. https://doi.org/10.1007/s41779- 021-00605-1.

[6] H.O. Tekin, F.T. Ali, G. Almisned, G. Susoy, S.A.M. Issa, A. Ene, W. Elshami, H.M.H. Zakaly, Multiple assessments on the gamma-ray protection properties of niobium-doped borotellurite glasses: A wide range investigation using monte carlo simulations, Sci. Technol. Nucl. Install. 2022 (2022) 1–17. https://doi.org/10.1155/2022/5890896.

[7] G. Almisned, H.O. Tekin, S.A.M. Issa, M.Ç. Ersundu, A.E. Ersundu, G. Kilic, H.M.H. Zakaly, A. Ene, Novel hmo-glasses with Sb_2O_3 and TeO_2 for nuclear radiation shielding purposes: A comparative analysis with traditional and novel shields, Materials (Basel). 14 (2021) 4330–4346. https://doi.org/10.3390/ma14154330.

[8] M.I. Sayyed, M. Çelikbilek Ersundu, A.E. Ersundu, G. Lakshminarayana, P. Kostka, Investigation of radiation shielding properties for MeO-$PbCl_2$-TeO_2 (MeO = Bi_2O_3, MoO_3, Sb_2O_3, WO_3, ZnO) glasses, Radiat. Phys. Chem. 144 (2018) 419–425. https://doi.org/10.1016/j.radphyschem.2017.10.005.

[9] A. Kumar, Gamma ray shielding properties of PbO-Li_2O-B_2O_3 glasses, Radiat. Phys. Chem. 136 (2017) 50–53. https://doi.org/10.1016/j.radphyschem.2017.03.023.

[10] E. Şakar, Ö.F. Özpolat, B. Alım, M.I. Sayyed, M. Kurudirek, Phy-X/PSD: Development of a user

friendly online software for calculation of parameters relevant to radiation shielding and dosimetry, Radiat. Phys. Chem. 166 (2020) 108496–108507. https://doi.org/10.1016/j.radphyschem.2019.108496.

[11] G. Battistoni, F. Cerutti, A. Fassò, A. Ferrari, S. Muraro, J. Ranft, S. Roesler, P.R. Sala, The FLUKA code: Description and benchmarking, AIP Conf. Proc., AIP, (2007) 31–49. https://doi.org/10.1063/1.2720455.

[12] N.A.M. Alsaif, H. Al-Ghamdi, H.M.H. Zakaly, M.H. Nasr, Y.S. Rammah, A.S. Abouhaswa, Nd_2O_3- doped borate/phosphate glasses for optical and radiation shielding applications: fabrication, physical, optical as well as gamma-ray attenuation capacity, Opt. Quantum Electron. 56 (2024) 552. https://doi.org/10.1007/s11082-023-06194-6.

[13] A. Kaur, A. Khanna, F. González, C. Pesquera, B. Chen, Structural, optical, dielectric and thermal properties of molybdenum tellurite and borotellurite glasses, J. Non. Cryst. Solids. 444 (2016) 1–10. https://doi.org/10.1016/j.jnoncrysol.2016.04.033.

[14] M. Rashad, H.O. Tekin, H.M. Zakaly, M. Pyshkina, S.A.M. Issa, G. Susoy, Physical and nuclear shielding properties of newly synthesized magnesium oxide and zinc oxide nanoparticles, Nucl. Eng. Technol. 52 (2020) 2078–2084. https://doi.org/10.1016/j.net.2020.02.013.

[15] G. Battistoni, T. Boehlen, F. Cerutti, P.W. Chin, L.S. Esposito, A. Fassò, A. Ferrari, A. Lechner, A. Empl, A. Mairani, A. Mereghetti, P.G. Ortega, J. Ranft, S. Roesler, P.R. Sala, V. Vlachoudis, G. Smirnov, Overview of the FLUKA code, Ann. Nucl. Energy. 82 (2015) 10–18. https://doi.org/10.1016/j.anucene.2014.11.007.

[16] A.M. Ali, S.A.M. Issa, M.R. Ahmed, Y.B. Saddeek, M.H.M. Zaid, M. Sayed, H.H. Somaily, H.O. Tekin, H.A.A. Sidek, K.A. Matori, H.M.H. Zakaly, Promising applicable heterometallic Al_2O_3/PbO_2 nanoparticles in shielding properties, J. Mater. Res. Technol. 9 (2020) 13956–13962. https://doi.org/10.1016/j.jmrt.2020.09.125.

[17] A. Ferrari, P.R. Sala, A. Fasso, J. Ranft, FLUKA: A Multi-Particle Transport Code, CERN-2005-10. (2005) INFN/TC 05/11, SLAC-R-773. https://doi.org/10.2172/877507.

[18] B.T. Tonguc, H. Arslan, M.S. Al-Buriahi, Studies on mass attenuation coefficients, effective atomic numbers and electron densities for some biomolecules, Radiat. Phys. Chem. 153 (2018) 86–91. https://doi.org/10.1016/J.RADPHYSCHEM.2018.08.025.

[19] M.S. Al-Buriahi, B.T. Tonguc, Mass attenuation coefficients, effective atomic numbers and electron densities of some contrast agents for computed tomography, Radiat. Phys. Chem. 166 (2020) 108507. https://doi.org/10.1016/j.radphyschem.2019.108507.

[20] J.S. Alzahrani, Z.A. Alrowaili, H.H. Saleh, A. Hammoud, S. Alomairy, C. Sriwunkum, M.S. Al-Buriahi, Synthesis, physical and nuclear shielding properties of novel Pb–Al alloys, Prog. Nucl. Energy. 142 (2021) 103992. https://doi.org/10.1016/J.PNUCENE.2021.103992.

[21] G. Kilic, E. Ilik, S.A.M. Issa, B. Issa, M.S. Al-Buriahi, U.G. Issever, H.M.H. Zakaly, H.O. Tekin, Ytterbium (III) oxide reinforced novel TeO_2–B_2O_3–V_2O_5 glass system: Synthesis and optical, structural, physical and thermal properties, Ceram. Int. 47 (2021) 18517– 18531. https://doi.org/10.1016/J.CERAMINT.2021.03.175.

[22] M.A. Alothman, I.O. Olarinoye, C. Sriwunkum, S. Alomairy, J.S. Alzahrani, M.S. Al- Buriahi, Study of the radiation attenuation properties of MgO-Al_2O_3-SiO_2-Li_2O-Na_2O glass system, J. Aust. Ceram. Soc. 58 (2022) 267–273. https://doi.org/10.1007/s41779-021-00687-x.

[23] A. Edukondalu, S. Stalin, M.S. Reddy, C. Eke, Z.A. Alrowaili, M.S. Al-Buriahi, Synthesis, thermal, optical, mechanical, and radiation-attenuation characteristics of borate glass system modified by Bi_2O_3/MgO, Appl. Phys.

DOI: 10.62184/mmc.jmmc110020242

Research Article

A. 128 (2022) 331. https://doi.org/10.1007/s00339-022-05475-3.

[24] S.A.M. Issa, Y.B. Saddeek, H.O. Tekin, M.I. Sayyed, K.S. Shaaban, Investigations of radiation shielding using monte carlo method and elastic properties of PbO-SiO_2-B_2O_3-Na_2O glasses, Curr. Appl. Phys. 18 (2018) 717-727. https://doi.org/10.1016/j.cap.2018.02.018.

[25] J.S. Alzahrani, Z.A. Alrowaili, C. Eke, Z.M.M. Mahmoud, C. Mutuwong, M.S. Al- Buriahi, Nuclear shielding properties of Ni-, Fe-, Pb-, and W-based alloys, Radiat. Phys. Chem. 195 (2022) 110090. https://doi.org/10.1016/j.radphyschem.2022.110090.